Title

Single-Pulse X-ray Acoustic Computed Tomographic Imaging for Precision Radiation Therapy

Journal

Advances in Radiation Oncology, 8(4)

ISSN

2452-1094

Authors

Gonzalez, Gilberto

Prather, Kiana

Pandey, Prabodh Kumar

et al.

Publication Date

2023-07-01

DOI

10.1016/j.adro.2023.101239

Peer reviewed

Advances in Radiation Oncology (2023) 8, 101239

advances in radiation oncology

www.advancesradonc.org

Scientific Article

Single-Pulse X-ray Acoustic Computed Tomographic Imaging for Precision Radiation Therapy

Gilberto Gonzalez, MS,[a] Kiana Prather, BS,[b] Prabodh Kumar Pandey, PhD,[c] Leshan Sun, MS,[d] Joseph Caron, MS,[a] Siqi Wang, MS,[d] Salahuddin Ahmad, PhD,[a] Liangzhong Xiang, PhD,[c,d,e,*] and Yong Chen, PhD, DABR[a,*]

[a]Department of Radiation Oncology, University of Oklahoma Health Sciences Center, Oklahoma City, Oklahoma; [b]University of Oklahoma College of Medicine, Oklahoma City, Oklahoma; [c]Department of Radiological Sciences, University of California, Irvine, California; [d]Department of Biomedical Engineering, University of California, Irvine, California; and [e]Beckman Laser Institute & Medical Clinic, University of California, Irvine, California

Received 8 February 2023; accepted 29 March 2023

Purpose: High-precision radiation therapy is crucial for cancer treatment. Currently, the delivered dose can only be verified via simulations with phantoms, and an in-tumor, online dose verification is still unavailable. An innovative detection method called x-ray −induced acoustic computed tomography (XACT) has recently shown the potential for imaging the delivered radiation dose within the tumor. Prior XACT imaging systems have required tens to hundreds of signal averages to achieve high-quality dose images within the patient, which reduces its real-time capability. Here, we demonstrate that XACT dose images can be reproduced from a single x-ray pulse (4 μs) with sub-mGy sensitivity from a clinical linear accelerator.

Methods and Materials: By immersing an acoustic transducer in a homogeneous medium, it is possible to detect pressure waves generated by the pulsed radiation from a clinical linear accelerator. After rotating the collimator, signals of different angles are obtained to perform a tomographic reconstruction of the dose field. Using 2-stage amplification with further bandpass filtering increases the signal-to-noise ratio (SNR).

Results: Acoustic peak SNR and voltage values were recorded for singular and dual-amplifying stages. The SNR for single-pulse mode was able to satisfy the Rose criterion, and the collected signals were able to reconstruct 2-dimensional images from the 2 homogeneous media.

Conclusions: By overcoming the low SNR and requirement of signal averaging, single-pulse XACT imaging holds great potential for personalized dose monitoring from each individual pulse during radiation therapy.

Sources of support: Research reported in this publication was supported by the National Cancer Institute of the National Institutes of Health (R37CA240806). The content is solely the responsibility of the authors and does not necessarily represent the official views of the National Institutes of Health. Approximately $500,000 of federal funds supported the effort (50%) on this project. Approximately $200,000 of American Cancer Society (133697−RSG−19−110−01−CCE) funds supported a portion of the effort (45%) on this project. The authors also acknowledge support from the University of California, Irvine Chao Family Comprehensive Cancer Center (P30CA062203) (5%).

Disclosures: The authors declare that they have no known competing financial interests or personal relationships that could have appeared to influence the work reported in this paper.

The data sets used and analyzed during the current study are available from the corresponding authors on reasonable request.

*Corresponding authors: Liangzhong Xiang, PhD; and Yong Chen, PhD, DABR; E-mails: liangzhx@hs.uci.edu yong-chen@ouhsc.edu

https://doi.org/10.1016/j.adro.2023.101239

Introduction

Radiation therapy has made significant strides in recent years with the development of advanced techniques such as intensity modulated radiation therapy,[1,2] stereotactic body radiation therapy,[3] and proton beam therapy.[4] These techniques have converged on the concept of precision radiation therapy, which aims to increase high-dose conformity, reduce planning target margins, and increase the dose to the tumor. However, delivering highly conformal treatments remains a significant challenge due to uncertainties in machine beam delivery and intrafractional changes in patient anatomy and tumor location during treatment (Fig. 1).[5,6]

To address this challenge, image guided radiation therapy solutions have been proposed, such as cone beam computed tomography (CT) and robotic couch, both of which are applied before treatment delivery to confirm the target position with respect to the isocenter.[7,8] However, these localization methods involve an additional imaging dose to the patient, and the uncertainty of the delivered radiation dose remains. There is currently no consensus on a standardized method for tracking the dose to the tumor in real time.[9] Thermoluminescent dosimeters have been used for individual point measurements of skin entrance dose,[10] but these methods do not provide real-time feedback. Electronic portal imaging devices[11] have also been considered for patient-specific quality assurance with high resolution; however, converting the transmitted fluence image to absolute dose is complex and requires several corrections for attenuation and scatter.

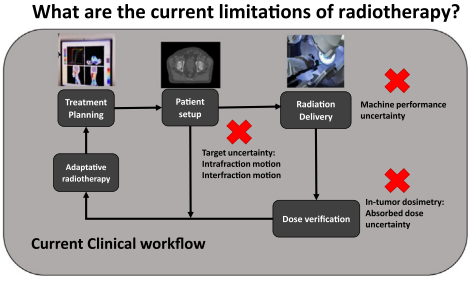

Figure 1 The workflow of radiation therapy. The patient's computed tomography (CT) simulation is used to create a treatment plan (eg, intensity modulated radiation therapy, arc therapy). With an approved plan, the patient will be placed in the treatment couch and be imaged before treatment delivery (cone beam CT or kV/MV x-rays). If the imaging (internal anatomy) does not agree with the CT simulation, a new simulation or replanning will be needed. There are several sources of uncertainty during treatment, such as target volume and normal tissue position within the patient, the performance of machine components during delivery, and the actual tumor dose delivered compared with the calculated treatment planning dose.

To address these challenges, a new method called x-ray acoustic CT (XACT) has been proposed. XACT is an alternative detection method that uses radiation-induced ultrasound emissions to provide real-time feedback on the delivered dose.[12] The reconstructed 2-dimensional (2D) XACT images can provide dosimetry information, and acoustic amplitude is linearly proportional to the absorbed dose in the medium.[13,14] This means that real-time mapping of dose distribution could become possible.

To progress into clinical application, novel transducers capable of dual-mode operation have been proposed for tracking both anatomy and delivered dose. A recent study shows the capability of real-time dose monitoring of a XACT/ultrasound (XACT/US) system,[15] demonstrating in vivo dual-mode mapping of 6X flattening filter-free (FFF) fields. However, a large number of beam pulses are required to improve image reconstruction, and the frame rate is still relatively slow, thus restricting intrafraction visualization of the treatment. This limitation can be overcome by achieving large signal-to-noise ratio (SNR) from a single-pulse acquisition. Further research is needed to improve the sensitivity and SNR of XACT and to develop transducers that operate in dual mode.[12,16] By overcoming these limitations, XACT shows promise in addressing organ motion and in-tumor relative dose evaluation. It could also provide feedback on machine performance, making it a valuable tool for precision radiation therapy. Current XACT systems require tens to hundreds of signal averages to achieve high-quality imaging, which restrains its real-time capability. Additionally, most studies rely on water phantoms as their propagation medium. The XACT signal is dependent on both the dose per pulse and the acoustic properties of the medium. Water has a low Grüneisen parameter, which makes it difficult to obtain a high signal SNR. The characterization of x-ray acoustic (XA) signals generated in tissues similar to the human body still needs to be investigated.

The purpose of this work is to demonstrate high SNR detectability for XACT imaging from the individual beam pulses from a clinical linear accelerator (linac). The irradiation was performed on a water phantom and a container with vegetable oil as a surrogate for fatty tissue. The influence of the Grüneisen parameter from both materials was explored and variation of collimator angles on SNR XACT amplitude and linearity response is compared between single-pulse and high-signal averaging mode. Finally, the clinical implementation of XACT, benefits, and further limitations are discussed.

Methods and Materials

Measurement of radiation dose with x-ray–induced acoustic emission

The acoustic effect of pulsed x-rays originates from photon-electron interactions that generate ionizations of the inner shell electrons. The released photoelectrons or Auger electrons are absorbed locally, which entails kinetic energy deposition. Given that clinical linac beams are typically used in the MV energy scale, Compton effect produces scattered electrons that also contribute to local energy deposition. This energy delivered to the medium translates into a temperature rise on a millikelvin (mK) scale, thus generating thermoelastic expansion. The expansion concludes with the emission and propagation of an acoustic pressure wave (Fig. 2).

The generated XA pressure wave can be described through the partial differential equation[12,17,18]

$$\nabla^2 p\left(\vec{r},t\right) - \frac{1}{v_s^2}\frac{\partial^2}{\partial t^2} p\left(\vec{r},t\right) = -\frac{\beta}{C_p}\frac{\partial}{\partial t} H\left(\vec{r},t\right), \quad (1)$$

where $H(\vec{r},t)$ is the x-ray heat energy deposition at point $\vec{r}$ and time t, v_s is the speed of sound in medium, β is the thermal expansion coefficient, and C_p is the specific heat capacity at constant pressure. The pressure wave equation can be simplified by assuming that each individual linac pulse deposits the heat energy instantaneously. Thus, the initial acoustic pressure wave $p_o(\vec{r})$ for a delta impulse is given by

$$p_o\left(\vec{r}\right) = \Gamma\, H\left(\vec{r}\right), \quad (2)$$

where Γ represents the Grüneisen parameter, a dimensionless term that compounds the thermoacoustic properties of a specific material or tissue. It is defined as

$$\Gamma = \frac{\beta v_s^2}{C_p} \quad (3)$$

The distribution of heat energy $H(\vec{r})$ can also be expressed in dosimetric terms, such as fluence F and x-ray mass energy absorption coefficient μ_{en}/ρ. Similarly, these terms can also be represented as thermal efficiency η_{th} (percentage of absorbed energy converted to heat) and dose per pulse D_p. The expression for initial pressure then can be described in different forms:

$$p_o\left(\vec{r}\right) = \frac{\Gamma\ (\mu_{en}/\rho)\ F}{\tau_p} = \frac{\Gamma\ \eta_{th}\rho\ D_p(r)}{\tau_p}, \quad (4)$$

where ρ is the mass density of the medium and $D_p(r)$ is the local dose due to a single x-ray pulse with a pulse duration of τ_p. The pixel intensity inside the XA image, which is reconstructed from acquired XA signals using backprojection, should correspond to the initial acoustic pressure. Therefore, the relative intensity of the XACT image reconstruction can provide information of beam position, dose distribution during the treatment delivery, and quantitative information on the amount of dose being delivered to the tumor target.

Experimental setup

Photon beams of varying square sizes were delivered using a TrueBeam linac (Varian Medical Systems, Palo Alto, CA). The beam energy used on all tests was 10 MV FFF with

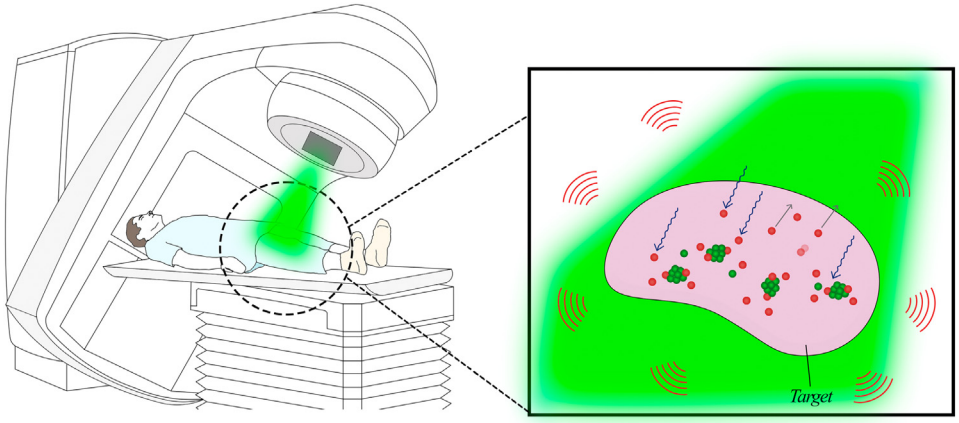

Figure 2 The x-ray acoustic effect from a linear accelerator photon beam. Pulsed x-ray beams deposit energy in the local target. This energy creates a rapid rise in temperature that is translated into mechanical vibrations, from which ultrasound waves can be detected, typically with acoustic transducers with central frequency of the kHz range. The initial pressure for these acoustic waves, under instantaneous energy deposition, is $p_o(\vec{r}) = \frac{\Gamma\ \eta_{th}\rho D_p(r)}{\tau_p}$; however, most clinical accelerators have beam pulses that have typical durations of 3 to 4 μs, which can degrade the acoustic peak resolution.

2400 MU per minute dose rate to implement the highest dose per pulse available. The linac pulse width has 4 μs duration and a repetition frequency of 360 Hz. The beams were delivered with different field sizes to assess the change in the XA signal peaks. An unfocused immersion-type transducer (V389-SU, Olympus-NDT, Waltham, MA) with 0.5 MHz central frequency was used to detect the acoustic signals in water and commercial vegetable oil. The transducer was fixed to a holder driven by the stepper motor of the water tank system (1D SCANNER, Sun Nuclear Corporation, Melbourne, FL). A distance of 10.5 cm between the transducer and the primary radiation field was used to avoid head-wave noise from scatter radiation. The XACT signals from the transducer passed through an initial stage preamplifier (5660B, Olympus-NDT) with 60 dB gain and −3 dB bandwidth from 20 kHz to 2 MHz. To reduce radiofrequency noise, copper foil was used to cover the transducer cable. A second stage amplifier (SR560, Stanford Research Systems, Sunnyvale, CA) added an additional gain and applied a bandpass filter. At last, the signal was collected by an oscilloscope that used the linac gun pulse for triggering. For single-pulse mode acquisitions, the total amplification was set to 90 dB with constrained bandpass cut-off frequencies of 10 kHz to 30 kHz with −6 dB. The sampling frequency was set to 250 MHz for a total of 70,000 collected datapoints per signal.

Single-pulse XACT signal characterization from 2 media

Acoustic signal detection was performed between 2 different Grüneisen parameter media. The literature suggests that, at room temperature, water has Γ of 0.11 whereas vegetable oil ranges between 0.90 to 0.95 depending on its contents. Initial testing compared the SNR and peak-to-peak voltage between both medium using only 60 dB gain and increasing the signal averages. Upon adjustments for single-pulse acquisitions, SNR was compared for different beam collimator angles of 0°, 15°, 30°, and 45°. The SNR was calculated for the time-domain signals as follows:

$$SNR\ [dB] = 20\log_{10}\left(\frac{\overline{I(t)}}{B(t)}\right)^2 \quad (5)$$

where $\overline{I(t)}$ represents the root-mean-square voltage of the first XA peak in the signal $I(t)$, whereas $B(t)$ is the remaining signal outside the XACT peaks. The higher SNR of XA signals in oil demonstrates that stronger acoustic signals could be obtained from a patient in future research without need for signal averaging.

XACT image reconstruction

The tomographic method requires acquiring signals from different angles, mimicking a ring-shaped array of transducers. In our experiments, the collimator was rotated every 5° for a total of 72 XACT signals (Fig. E1 in Supplementary material). The background signals were obtained by withholding the beam-on, which allows for linac gun triggers to be sent to the oscilloscope without performing actual beam delivery. A backprojection script was used with MATLAB to reconstruct the radiation-induced initial pressure distribution. The script reads each of the .csv files from a folder directory, then separates the data into 2 arrays for the trigger signal and the transducer signal, respectively. For each of the 72 measurement angles, the signal obtained from the background is subtracted, and a Savitsky-Golay filter is applied. Subsequently, the dimensions of the reconstruction's domain of interest and the grid resolution for the forward model (in our case, 0.25 mm) are defined. The domain is discretized with the Delaunay function, and the detectors are defined in a circle of radius corresponding to the distance between the transducer and the beam isocenter. The contribution of each of the 72 points from the time-of-flight from the signals are obtained, considering a velocity in homogeneous medium of 1500 m/s in water and 1420 to 1450 m/s in oil. The net contribution is used to generate a surface plot in 2D.

Imaging of the radiation field and a high-density target

We introduced a high-density material within the oil to take advantage of the increased Grüneisen parameter. A small 7-mm diameter cerrobend rod was placed in the isocenter of a 5- × 5-cm^2 field. An Olympus transducer with 2.25 MHz central frequency was used for this test, and a single-pulse XACT reconstruction was obtained.

Linearity response

The linear response of the XACT intensity was compared as the transducer was introduced deeper into the water tank. Measurements were made from 3.5 cm to 12 cm depth taking 5 mm steps. Normalization was performed with respect to the first measurement point, and a scaling factor was used to plot the percentage depth dose from the clinical commissioned data. The mean response and standard deviation were plotted for single-pulse XACT and 1024 averages.

Results

Detection of a single x-ray beam pulse with XACT

Single-pulse XACT signals recorded for a field size of 4 × 4 cm^2 are shown in Fig. 3a. The peak-to-peak

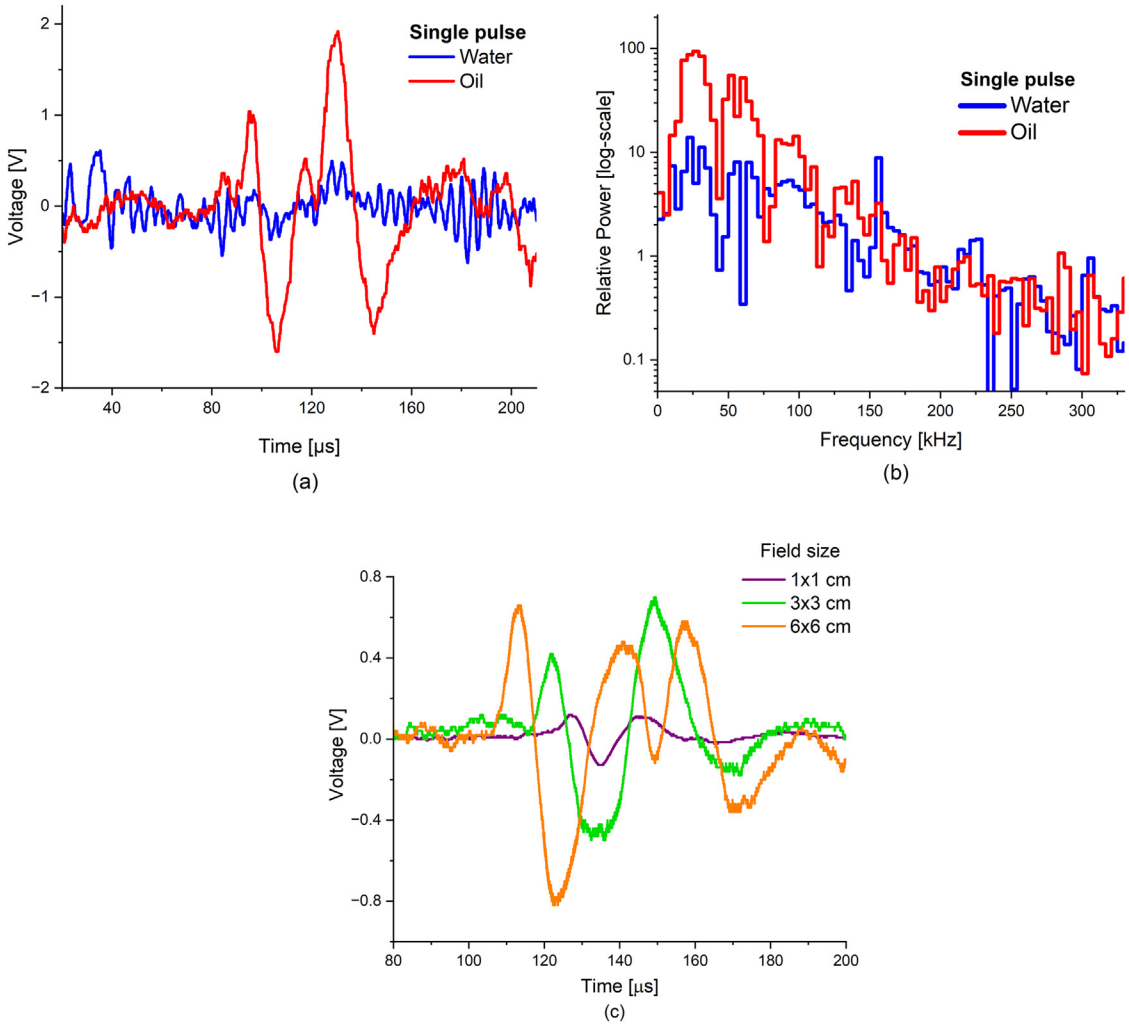

Figure 3 X-ray–induced acoustic computed tomography (XACT) signal acquisitions. (a) The time-domain XACT signal for both oil and water medium using a single beam pulse. (b) The frequency spectrum of the single-pulse XACT signals. Most of the sensitivity uptake lies at the lower frequencies (peaks at 25 kHz and 50 kHz). (c) The effect of increasing the field size for single-pulse XACT in oil. As field increases on X-dimension, there is a larger number of pressure sources created in front of the transducer, thus increasing amplitude. As Y-dimension is modified, it affects the distance between field edge and the transducer, therefore affecting the travel time of the signals.

amplitude of the acoustic waves generated from oil is 5 to 6 times greater than that of water due to the Grüneisen parameters Γ, which are approximately 0.11 for water and 0.90 for oil. Time-of-flight calculations can determine the photon field size. The time between the first peak's compression-rarefaction and the second peak is used to determine the closest result to the actual field size. For water, the timepoints are 101.4 μs and 129.8 μs, while for oil, they are 99.8 μs and 130.2 μs. By considering the speed of sound in water and oil, an estimated distance of 4.20 cm in water and 4.31 cm in oil can be obtained. However, these are rough approximations due to the field divergence at the 5-cm depth of measurement. The frequency spectrum in Fig. 3b shows that signal uptake is dominant for lower frequencies, with sensitive peaks at 25 kHz and 50 kHz for both media. From the first acoustic peak, the SNR and peak-to-peak voltage were recorded, and it was found that in water, 16 averages were necessary to satisfy a SNR > 5. In contrast, using averaging was unnecessary in oil. These results suggest that structures with large Grüneisen parameters may not require signal averaging to be identified in XACT for future heterogeneous phantom studies. Table 1 summarizes the results obtained using only 1 amplifier stage.

A secondary amplification stage enhanced the acoustic signal so that higher SNR was achieved in both propagation media. Rotating the beam collimator caused the pressure source line (edge of field) to no longer be similarly aligned toward the face of the transducer. In all cases, the more oblique angles had reduced SNR. This is because the arrival time of the pressure wave is different along the rotated source. Despite this limitation, XACT from oil

Table 1 SNR and voltage values from 1-stage amplifier XACT first acoustic peak as a function of signal averaging (beam pulses) in 2 different media*

One-stage amplification	Water		Vegetable oil	
Γ at 20°C	0.11		0.90	
Signal averages	Peak-to-peak (V)	SNR	Peak-to-peak (V)	SNR
2	0.56	1.7	1.32	17.0
8	0.27	3.2	1.10	19.1
16	0.28	5.5	1.30	19.4
32	0.21	6.1	1.22	20.6
64	0.23	9.3	1.24	20.1
128	0.23	10.2	1.24	20.2
256	0.20	10.7	1.22	19.2
512	0.20	10.9	1.22	20.6
Two-stage amplification	**Water**		**Vegetable oil**	
Collimator angle (°)	SNR at 4 cm (0.5 MHz)	SNR at 8 cm (0.5 MHz)	SNR at 4 cm (0.5 MHz)	SNR at 4 cm (2.25 MHz)
0	5.82	5.56	8.99	7.29
15	6.03	5.46	8.03	6.70
30	4.00	3.82	6.06	4.93
45	3.35	3.76	6.28	5.25

Abbreviations: SNR = signal-to-noise ratio; XACT = x-ray–induced acoustic computed tomography.
* The properties influencing the Grüneisen parameter, $\Gamma = \frac{\beta v_s^2}{C_p}$, are related to the initial pressure strength. The SNR for the acoustic peaks detected with 2-stage amplification (for single beam pulse mode) are recorded at 2 depths for a 0.5 MHz and a 2.25 MHz transducer.

satisfied the Rose criterion SNR for all acquisitions using the 0.5 MHz transducer.

Single-pulse XACT signals can provide information on the dose distribution or shape of the treatment field. This is observed in Fig. 3c for XACT in oil from square fields with sides of 1 cm, 3 cm, and 6 cm. The distance between the transducer and the isocenter is maintained, so increasing the field size on Y-direction causes one edge of the field to move closer to the transducer as the opposite edge moves away. Therefore, the temporal position of the second peak becomes delayed and attenuated. Simultaneously, varying the X-dimension modifies the acoustic amplitude because the number of pressure sources are increased along that field edge.

2D XACT dose images from single-pulse acquisition

Two-dimensional XACT images were obtained from simple backprojection of the processed single-pulse acoustic signals. The intensity profile of the reconstructed 5- × 5-cm^2 field in water is displayed for Fig. 4a. Grain-like artifacts are observed for the background region surrounding the field; this is attributed to the low SNR in water. The intensity profiles show that flatness is better preserved in oil in Fig. 4b, whereas for water there are signs of inhomogeneities in the central region. The full-width half maximum of both intensity profiles is close to the actual field size: 5.10 × 4.88 cm^2 in water and 5.05 × 4.97 cm^2 in oil. However, the penumbra has a sharper gradient in the single-pulse image for oil. In similarity to clinical dose profiles, these profiles show the distinctive horns on the lateral edges, which can be observed in typical lateral beam profiles at similar depths. Figure 4c shows the reconstruction from a pyramid multileaf collimator plan for field sizes of 3 cm and 5 cm. The XACT images did not show the higher intensity that FFF-beam energy profiles have at the central region. This is a limitation of the simple backprojection reconstruction.

XACT of the photon field and a high-density target with a higher frequency transducer

Single-pulse XACT reconstruction from a higher frequency transducer was tested: a cylinder rod of cerrobend metal with length of 4 cm and diameter of 7 mm was placed at the isocenter of a 5- × 5-cm^2 field. The time domain signal is shown in Fig. 5a. To compare the 2

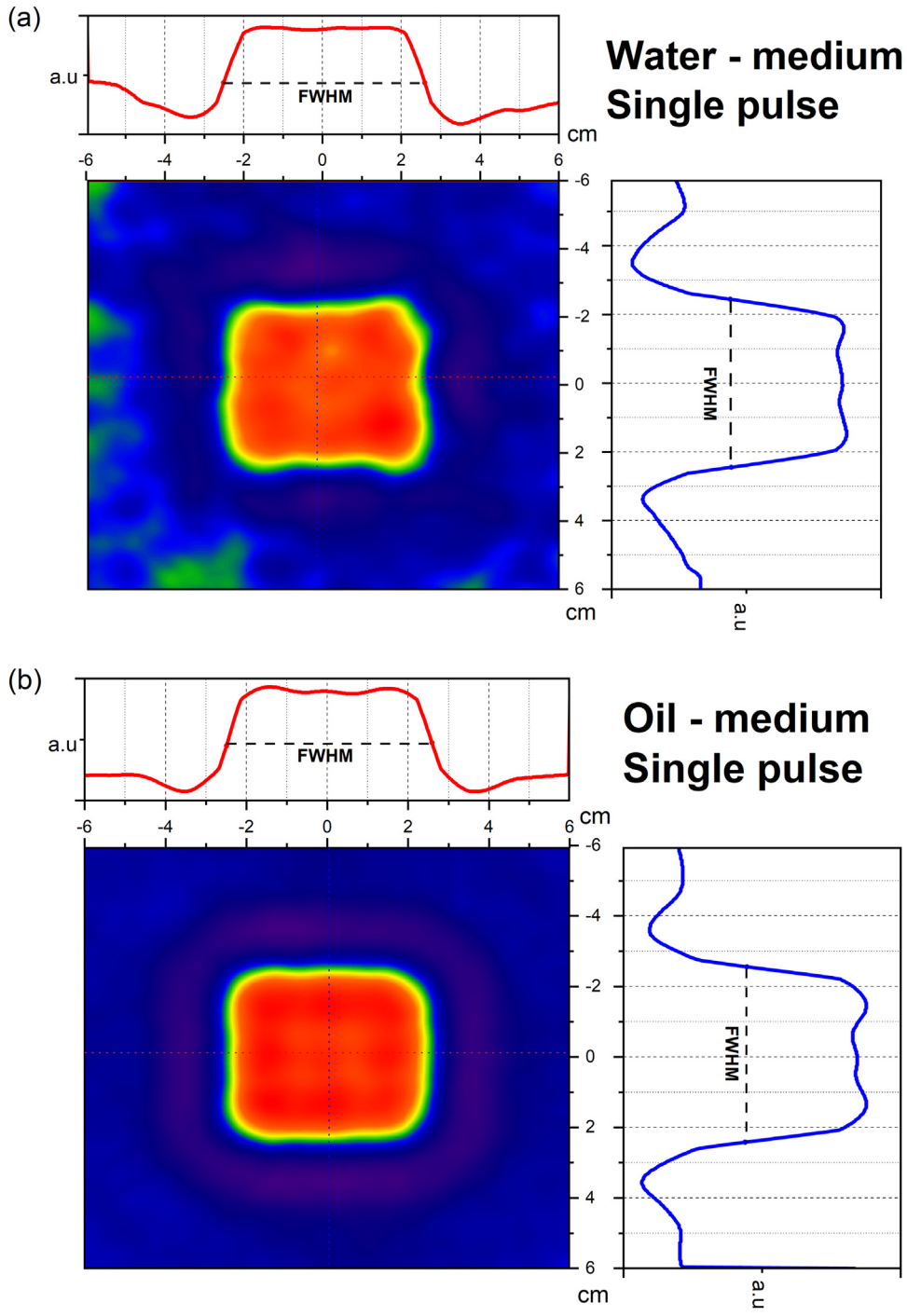

Figure 4 The beam's flatness and symmetry are represented with 2-dimensional x-ray–induced acoustic computed tomography (XACT) intensity profiles. (a) Field (5×5 cm^2) in water using single-pulse acquisition mode. (b) Field (5×5 cm^2) in vegetable oil using single-pulse acquisition mode. The reconstruction full-width half maximum (FWHM) of the profiles is 5.10×4.88 cm^2 in water and 5.05×4.97 cm^2 in oil. The penumbra, defined by the fall-off region from 80% to 20% intensity, has a sharper gradient in the single-pulse image for oil. Similar to clinical profiles, these XACT-based profiles show the distinctive horns on the lateral edges, which can be observed in typical lateral beam profiles at similar depths. (c) Two-dimensional XACT of multileaf collimator–pyramid plan, with representation of 3 cm and 5 cm field sizes. However, both acquisitions did not show the higher intensity that flattening filter-free beam energy profiles have at the central region, which is a limitation of the simple backprojection reconstruction.

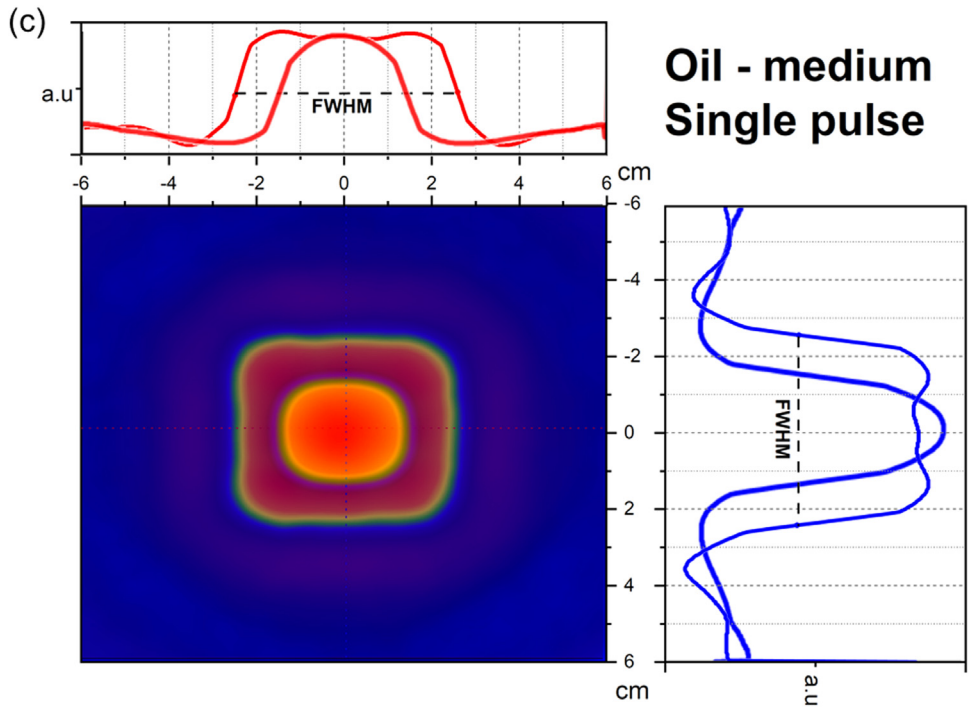

Figure 4 **Continued.**

transducers, the normalized frequency spectrum of single-pulse XACT using both transducers is shown in Fig. 5b. The spectrums show the XA signal predominates around 30 kHz; however, there is considerable uptake at 150 kHz and 300 kHz, which can provide additional information about the object in the field. In general, adding the presence of a high-density material can result in higher frequency signal components. The frequency spectrum of XACT is dependent on the specific geometry and properties of the high-density material, the x-ray energy, field shape, dose rate, and the acoustic properties of the medium. Finally, Fig. 5c illustrates the image reconstruction of the field and the cerrobend rod. The profile presented a distortion due to the metallic rod causing the full-width half maximum to be reduced compared with the previous result in Fig. 4b.

XACT linear response

A linear response was obtained by measuring the intensity of the acoustic peak as the transducer descended in the water tank up to 12 cm. The peak-to-peak voltage was normalized to the clinical percent depth-dose from the treatment planning software. Five measurements were made to obtain a mean and standard deviation for the single-pulse XACT. Similarly, mean values were obtained using 512 averages for comparison (Supplementary material).

Discussion

Acoustic imaging with x-rays has shown great potential as an in vivo dosimetry tool for radiation therapy. The ability to monitor and visualize radiation dose in real time using XACT could greatly improve the accuracy and precision of radiation delivery. However, current radiation-acoustic systems are limited by low SNR, which limits their potential: obtaining high SNR from a single beam pulse is the foundation for real-time acquisition. Each beam pulse has a particular amount of dose and distribution within the patient, and the collection of pulses constitutes the treatment beam. Even with the development of fast reconstruction algorithms or large element transducers, high SNR is still required for reconstructing dose of individual pulses in real time. Toward this goal, this work demonstrates that XACT can achieve 2D images of photon fields from a single linac beam pulse with sub-mGy sensitivity.

XACT imaging using a single pulse is challenging in water due to its low Grüneisen parameter, resulting in lower SNR. However, in a clinical setting, tissues produce varying acoustic intensities under the same radiation beam[19] because of their specific Grüneisen parameter and densities. Previous studies have experimentally determined Grüneisen parameters for various biologic tissues such as lipids, serum, red blood cells, fat, and bone.[20] This work used vegetable oil as a surrogate for fatty tissue, and results show that XACT from oil has 1.5 times greater

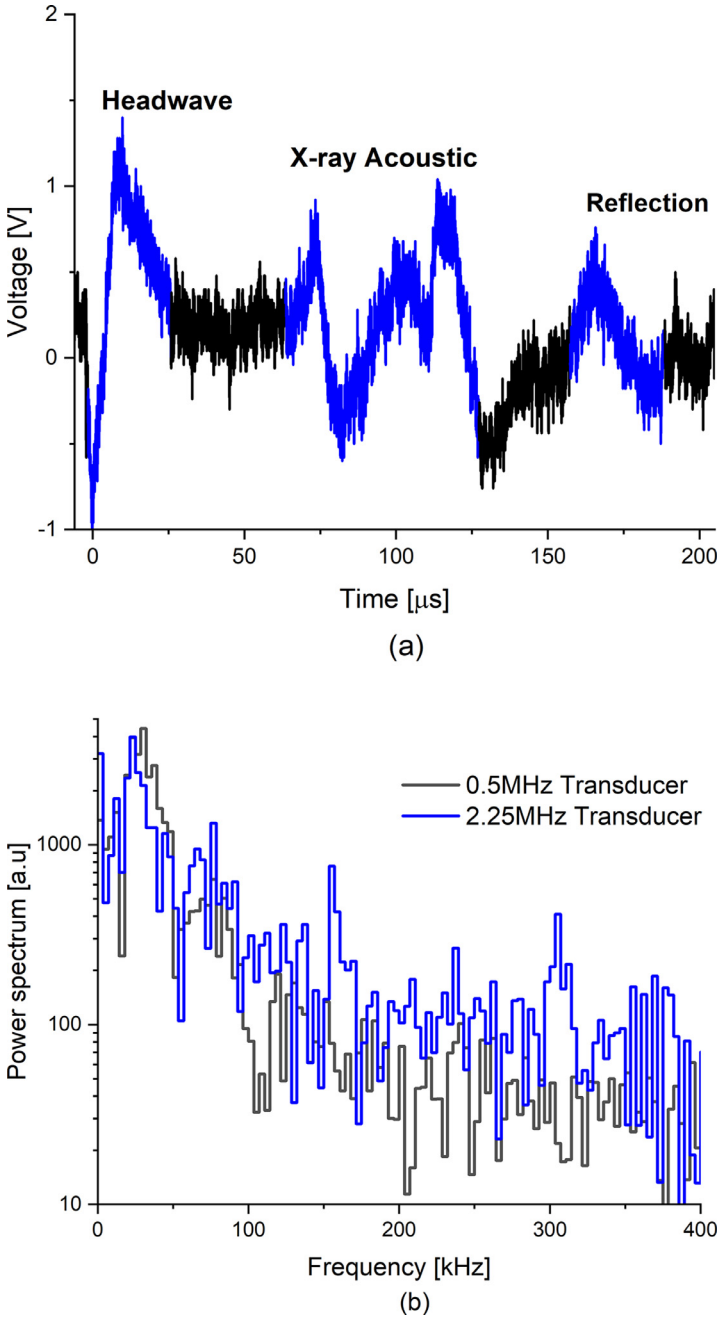

Figure 5 Single-pulse x-ray–induced acoustic computed tomography (XACT) with a 2.25 MHz central frequency transducer. (a) Single-pulse XACT using a higher frequency transducer. Despite possessing low sensitivity for the kHz range of the XA waves, using 2-stage amplification with sufficient gain and filtering allows for increased signal-to-noise ratio. (b) The frequency spectrum for both transducers possesses sensitivity uptake prominent at 20 kHz to 30 kHz; however, there is considerable uptake at 150 kHz and 300 kHz for the 2.2 MHz transducer. (c) The 2-dimensional XACT reconstruction with a cerrobend rod at the isocenter of a 10 MV flattening filter-free field. Abbreviation: FWHM = full-width half maximum.

SNR than water for single-pulse acquisitions. Since human tissues possess a larger Grüneisen parameter than water, high-signal averaging may not be necessary.

To implement XACT for in vivo dosimetry, transducers must be positioned strategically to avoid treatment fields. The transducers can be placed at the patient's CT simulation to design treatment plans that do not interfere with XACT/US acquisition.[12,18] However, this can be challenging in some cases, such as modulated arc therapy. Single-element transducers cannot reconstruct 2D/3D

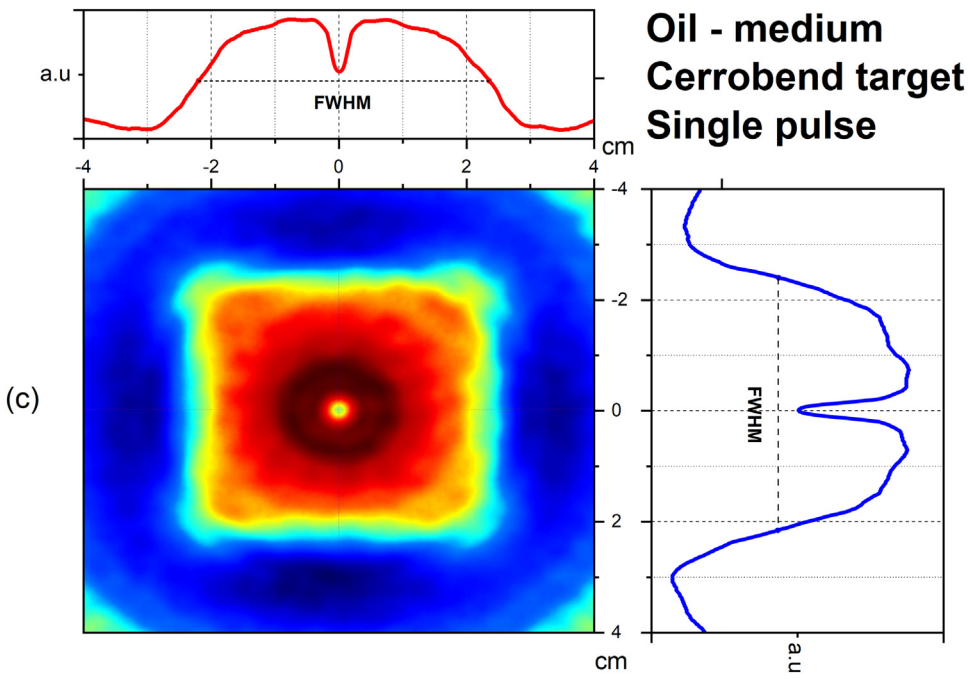

Figure 5 **Continued.**

information unless they scan around the patient, and a ring-type array may have reduced acquisition time but can be difficult to fix around the patient.[21] To progress to a clinical setting, further studies have to be performed for tissue-mimicking phantoms to characterize the quality of XACT signals. XACT/US systems should consider the medium's acoustic properties and adjust their amplifier gain and filtering to increase signal quality. Thus, a bidimensional transducer array capable of performing single-pulse XACT in synergy with dual ultrasound acquisition for coregistration should be developed and tested in the future.

XACT can be used to monitor treatments where there is a risk of high dose spread from the target volume to normal tissue, particularly stereotactic body radiation therapy treatments with FFF photon energies. Depending on the agreement between intrafractional anatomy and delivered dose imaging, there could be plan readaptation for subsequent fractions. Another promising application is dosimetry for FLASH therapy,[16] where beam pulse structure is striving toward ultrashort high dose rates. XACT can potentially solidify its position as a dosimetric tool for FLASH therapy as higher dose per pulse can considerably increase SNR, and the shorter beam pulse can improve spatial resolution. A recent study reported the experimental demonstration of XACT of a high-resolution target using a single pulse of 50 ns, achieving a resolution of 0.97 mm, exhibiting the growing benefits of these ultrafast radiation pulses.[22]

An alternative to enhance to acoustic signal involves photoacoustic contrast agents or gold nanoparticles, although this has been studied toward proton-induced acoustics for range verification.[23] Using high-density markers can improve the SNR. In this work, we aimed to show that even high-frequency transducers, which are far from the range of the XA effect (tens of kHz), can perform single-pulse XACT with targets in the field. The introduction of a high-density object can generate an increase in SNR and alter the spectrum of detected frequencies. We were able to reconstruct an image of the field at the same time as the cerrobend rod at the isocenter. Potentially, XACT/US systems can be further adapted to image radiation dose along with fiducial markers, such as in prostate cases, for real-time monitoring.

Finally, it is worth noting that this work was performed in early-stage conditions using a simple backprojection reconstruction method. For accurate dose reconstruction, the algorithm requires information about acoustic propagation in heterogeneous medium, physical modeling of the transducer, and the machine beam source. In future research, model-based algorithms[24] can take advantage of single-pulse XACT to progress toward real-time quantitative dosimetry.

Conclusion

This work demonstrated the feasibility of obtaining XACT dose images from a single linac beam pulse. The XA signal SNR depends on multiple factors such as the amplification stages of the detection system, the characteristics of the beam pulse, and the acoustic properties of the

irradiated medium. Further development of single-pulse XACT array systems will be crucial for real-time monitoring in the clinic and further studies will require characterizing acoustic signals from heterogeneous media.

Supplementary materials

Supplementary material associated with this article can be found in the online version at doi:10.1016/j.adro.2023.101239.

References

1. Cheung KY. Intensity modulated radiotherapy: Advantages, limitations and future developments. *Biomed Imaging Interv J*. 2006;2:e19.
2. Shimizuguchi T, Nihei K, Okano T, Machitori Y, Ito K, Karasawa K. A comparison of clinical outcomes between three-dimensional conformal radiotherapy and intensity-modulated radiotherapy for prostate cancer. *Int J Clin Oncol*. 2017;22:373-379.
3. Brandner ED, Chetty IJ, Giaddui TG, Xiao Y, Huq MS. Motion management strategies and technical issues associated with stereotactic body radiotherapy of thoracic and upper abdominal tumors: A review from NRG oncology. *Med Phys*. 2017;44:2595-2612.
4. Paganetti H, ed. *Proton Therapy Physics*. 2nd ed. Boca Raton, FL: CRC Press; 2019.
5. Bertholet J, Knopf A, Eiben B, et al. Real-time intrafraction motion monitoring in external beam radiotherapy. *Phys Med Biol*. 2019;64:15TR01.
6. Tong X, Chen X, Li J, et al. Intrafractional prostate motion during external beam radiotherapy monitored by a real-time target localization system. *J Appl Clin Med Phys*. 2015;16:51-61.
7. Dang A, Kupelian PA, Cao M, Agazaryan N, Kishan AU. Image-guided radiotherapy for prostate cancer. *Transl Androl Urol*. 2018;7:308-320.
8. Park J, Yea JW, Park JW, Oh SA. Evaluation of the setup discrepancy between 6D ExacTrac and cone beam computed tomography in spine stereotactic body radiation therapy. *PLoS One*. 2021;16:e0252234.
9. International Atomic Energy Agency. *Accuracy Requirements and Uncertainties in Radiotherapy*. Vienna, Austria: International Atomic Energy Agency; 2016.
10. Mijnheer B, Beddar S, Izewska J, Reft C. In vivo dosimetry in external beam radiotherapy. *Med Phys*. 2013;40: 070903.
11. Nailon WH, Welsh D, McDonald K, et al. EPID-based in vivo dosimetry using Dosimetry Check^{TM}: Overview and clinical experience in a 5-yr study including breast, lung, prostate, and head and neck cancer patients. *J Appl Clin Med Phys*. 2019;20:6-16.
12. Hickling S, Xiang L, Jones KC, et al. Ionizing radiation-induced acoustics for radiotherapy and diagnostic radiology applications. *Med Phys*. 2018;45:e707-e721.
13. Hickling S, Hobson M, El Naqa I. Characterization of x-ray acoustic computed tomography for applications in radiotherapy dosimetry. *IEEE Trans Radiat Plasma Med Sci*. 2018;2:337-344.
14. Xiang L, Tang S, Ahmad M, Xing L. High resolution x-ray-induced acoustic tomography. *Sci Rep*. 2016;6:26118.
15. Zhang W, Oraiqat I, Lei H, Carson PL, El Naqa I, Wang X. Dual-modality x-ray-induced radiation acoustic and ultrasound imaging for real-time monitoring of radiotherapy. *BME Frontiers*. 2020 9853609.
16. Oraiqat I, Zhang W, Litzenberg D, et al. An ionizing radiation acoustic imaging (iRAI) technique for real-time dosimetric measurements for FLASH radiotherapy. *Med Phys*. 2020;47:5090-5101.
17. Xiang L, Han B, Carpenter C, Pratx G, Kuang Y, Xing L. X-ray acoustic computed tomography with pulsed x-ray beam from a medical linear accelerator. *Med Phys*. 2013;40: 010701.
18. Samant P, Trevisi L, Ji X, Xiang L. X-ray induced acoustic computed tomography. *Photoacoustics*. 2020;19: 100177.
19. Patch SK, Nguyen C, Dominguez-Ramirez D, et al. Thermoacoustic range verification during pencil beam delivery of a clinical plan to an abdominal imaging phantom. *Radiother Oncol*. 2021;159:224-230.
20. Yao DK, Zhang C, Maslov K, Wang LV. Photoacoustic measurement of the Gruneisen parameter of tissue. *J Biomed Opt*. 2014;19:17007.
21. Tang S, Nguyen DH, Zarafshani A, et al. X-ray-induced acoustic tomography with an ultrasound ring-array. *Appl Phys Lett*. 2017;110: 103504.
22. Wang S, Ivanov V, Pandey PK, Xiang L. X-ray-induced acoustic computed tomography (XACT) imaging with single-shot nanosecond x-ray. *Appl Phys Lett*. 2021;119: 183702.
23. Takayanagi T, Uesaka T, Kitaoka M, et al. A novel range-verification method using ionoacoustic wave generated from spherical gold markers for particle-beam therapy: A simulation study. *Sci Rep*. 2019;9:4011.
24. Pandey PK, Wang S, Aggrawal HO, Bjegovic K, Boucher S, Xiang L. Model-based x-ray-induced acoustic computed tomography. *IEEE Trans Ultrason Ferroelectr Freq Control*. 2021;68:3560-3569.